Journal of Engineering and Applied Science Vol. 08, No. 02, pp. 72–80, December 2024

Journal of Engineering and Applied Science

Contents are available at www.jeas.ruet.ac.bd

Active Vibration Isolation System with Active Dynamic Vibration Absorber Using Kalman Filter Estimated Acceleration Feedback

Syed Mamun R Rasid[1*], Md. Abdul Kader[1], Mhia Md. Zaglul Shahadat[1], Md. Emdadul Hoque[1], Takeshi Mizuno[2]

[1]*Department of Mechanical Engineering, Rajshahi University of Engineering and Technology, Bangladesh.*
[2]*Department of Mechanical Engineering, Saitama University, Japan.*

ARTICLE INFORMATION

Received date: 30th Sep 2024
Revised date: 15th Dec 2024
Accepted date: 27th Dec 2024

Keywords

Active Vibration Isolation
Active dynamic Vibration Absorber
Kalman Filter
PID controller

ABSTRACT

An active vibration isolation system has been developed using an Active Dynamic Vibration Absorber (ADVA) that functions as an accelerometer in the high-frequency domain. The system employs an air spring to suspend the isolation table, serving as the control unit in the low-frequency region, while the ADVA controls high-frequency vibrations. The movements of the isolation table and the ADVA's absorber mass are regulated by a PID controller, with additional acceleration feedback enhancing isolation characteristics. Instead of costly servo-accelerometer or a noisy Micro-Electro-Mechanical Systems (MEMS) accelerometer, the acceleration of the isolation table is estimated using a Kalman Filter. The Kalman Filter-estimated acceleration is more accurate and less noisy than the ADVA-estimated acceleration. This estimated acceleration is integrated with PID control for the vibration control of the isolation table. Experimental results demonstrate significant performance improvements. The resonance peak of the isolation table is reduced from -64.65 dB to -73.58 dB, indicating a two-fold reduction and shorter settling time compared to ADVA-estimated acceleration feedback. In terms of vibration transmissibility, the resonance magnitude decreases from 12 dB to 3 dB. These results confirm that Kalman Filter-estimated acceleration enhances vibration isolation effectiveness and offers a cost-effective alternative to servo-type accelerometers.

1. Introduction

Vibration isolation has emerged as a critical area of research in several mechanical systems and sectors, such as silicon wafer fabrication, high-precision measurement instruments, aerospace technologies, and semiconductor manufacturing [1-6]. It is essential that these systems remain devoid of vibrations caused by direct disturbances and ground vibrations concurrently [7]. Passive and active vibration isolation are two prevalent methods for mitigating vibration. A popular and recognised passive vibration isolation method incorporates passive components, such as metal springs [8] and springs [8], to reduce vibrations.

* Corresponding authors: Department of Mechanical Engineering, Rajshahi University of Engineering & Technology, Bangladesh
E-mail addresses: mamun@me.ruet.ac.bd (Syed Mamun R Rasid)

However, the effectiveness of passive vibration isolations is restricted by inadequate performance in the low-frequency range [9, 10].

In contrast, active vibration isolation devices systems may overcome these limitations [11-14]. In the past, numerous approaches used to set up active vibration isolation systems [15-17].The arrangement of two isolators in series is an effective approach for sustaining parallel high-stiffness and low-stiffness suspension systems [18-20]. High-stiffness and low-stiffness components are combined to achieve zero displacement under on-board disturbances and ground vibrations. The positive and negative stiffness are combined to achieve zero displacement in response to both on-board disturbances and ground vibrations. A linear dynamic vibration absorber has been integrated with the isolation table to create a quasi-zero stiffness (QZS) vibration isolation system [21, 22].

A variety of control algorithms, such as state feedback [23], H∞ control [24], feedforward control [25], repetition [26], active acceleration control [27, 28], and PID control [29], robust control [30, 31] have been applied to develop an active isolation system. In order to detect low-frequency vibrations, all active system control methods necessitate high-performance sensors, such as servo-type accelerometers, which can be costly [32]. A high-speed valve is required for a pneumatic actuator to achieve better performance [33] in low-frequency region. The high cost of these components becomes the primary barrier to the widespread application of active isolation systems in industrial production processes.

MEMS accelerometers act as a cost-effective alternative for commercial servo-accelerometers in the detection of acceleration[34, 35]. In contrary to servo accelerometers, MEMS accelerometers show less sensitivity in the low-frequency band [36]. Moreover, additional noise in MEMS accelerometers at frequencies that are low adversely affects dynamic responses [37]. The active vibration isolation system integrates an active dynamic vibration absorber (ADVA), serves as an acceleration sensor in the low-frequency area and a MEMS accelerometer in the high-frequency region [28]. The sensor fusion strategy [38] combines low-frequency and high-frequency acceleration signals and applied with PID control as additional feedback to enhance performance of isolation. However, the technique used for obtaining a broad range of acceleration signals is highly complicated. The selection of the cut-off frequency of high-pass and low-pass filters in sensor fusion method affects the acceleration signal and influences the dynamic characteristics of the isolation table.

In this paper, Kalman filter is used to estimate the acceleration from the direct measurements instead of expensive servo accelerometers and noisy MEMS accelerometer. The estimated acceleration is compared with the acceleration captured from ADVA's control input in the low-frequency band. It is then used as additional feedback with PID control to improve the vibration isolation characteristics. A number of experiments were conducted to measure the dynamic characteristics such as compliance and transmissibility and the effect of the Kalman filter estimated acceleration on the dynamic characteristics of the table. The performance of the ADVA's estimated acceleration and Kalman filter estimated acceleration are compared in terms of dynamic characteristics.

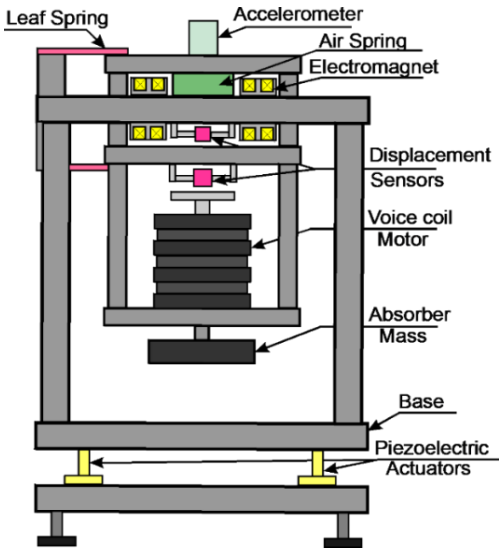

(a)

(b)

Figure 1. (a) Schematic of the developed system (b) fabricated

2. Structure of the Active vibration isolation system

The developed active vibration isolation system is depicted in the Figure 1. The system consists of a mass (m_1) of the isolation table that is supported by a spring (k_1) and a damper (c_1). Both low-frequency positioning and vibration control are performed by the pneumatic actuator. The absorber mass (m_2) hangs from the isolation table and a Voice Coil Motor (VCM) control the motion of the ADVA's mass. A displacement sensor S_1under the isolation table measures the relative motion of the isolation table in relation to the base, whilst another sensor S_2 measures the relative displacement of the absorber mass with respect to the isolation table. The servo-types of accelerometers and MEMS accelerometer are mounted on the isolation table. The high-frequency acceleration of the table is measured using an inexpensive MEMS sensor (S_a), while the low-frequency acceleration can be calculated from the VCM's control current.

3. Principles of Active Dynamic Vibration Absorber

Figure 2 illustrates the schematic diagram of the active dynamic vibration absorber employed in the proposed active vibration isolation system. The primary purpose of the ADVA is to reduce the vibration of the isolation table. The ADVA's mass exhibit in-phase movement with the isolation table in the low-frequency area and out-of-phase motion in the high-frequency region. As a result, it primarily operates as a control device in the high-frequency domain.

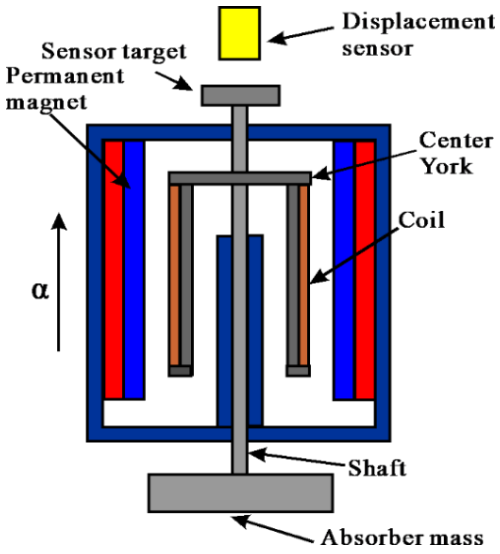

Figure 2. Structure of the ADVA

The ADVA's construction mimics that that of a servo-accelerometer, which facilitates the estimation of low-frequency acceleration from ADVA control current. The formula for calculating acceleration is provided in [28].

4. Modelling and Controller Design

Mathematical modelling

The equations of motion of the isolation table and the ADVA's mass can be expressed as follows:

$$m_1\ddot{x}_1 = -k_1y_1 - c_1\ddot{y}_1 + k_si_1 - k_2i_2 + f_a + f_d \quad (1)$$

$$m_2\ddot{x}_2 = k_2i_2 \quad (2)$$

where $m_1$represents the mass of the isolation table, x indicates displacements, f_a: force generated by the pneumatic actuator, f_v: ADVA's control force, f_d: force caused by the direct disturbance. Also, the subscript 0, 1, 2 identifies the base, vibration table and ADVA's mass.

The force fa is represented by

$$f_a = A_0p(t) \quad (3)$$

where A_0: cylinder area, p: compressed air pressure. The pressure of the compressed air satisfies the following equation

$$T\frac{dp(t)}{dt} + p(t) = k_si_1(t) \quad (4)$$

where k_s: valve coefficient, T: time constant, i_1: control current of the valve.

By applying the Laplace transform to the equations (1)-(4), the following equations are obtained:

$$m_1s^2X_1(s) = -k_1Y_1(s) - c_1sY_1(s) + k_sI_1(s) - k_2I_2(s) + F_a(s) + F_d(s) \quad (5)$$

$$m_2s^2X_2(s) = k_2I_2(s) \quad (6)$$

$$F_a = A_0P(s) \quad (7)$$

$$TsP(s) + P(s) = k_sI_1(s) \quad (8)$$

The control current of PID controller, including additional acceleration feedback for the isolation table and ADVA mass, can be written as follows:

$$I_1(s) = -\left(K_{p1}Y_1(s) + K_{i1}\frac{Y_1(s)}{s} + sK_{d1}Y_1(s)\right) - s^2G_F(s)K_{a1}X_1(s) \quad (9)$$

$$I_2(s) = -\left(K_{p2}Y_2(s) + K_{i2}\frac{Y_2(s)}{s} + sK_{d2}(s)Y_2(s)\right) \quad (10)$$

where, $Y_1 = (X_1 - X_0)$ is the displacement of the table with respect to the base; $Y_2 = (X_2 - X_1)$ is the displacement of the ADVA's mass to relative to the isolation table, P_p is proportional, P_d is derivative, P_i is integral, P_v and P_a is gains of acceleration feedback.G_F denotes the low pass filter transfer function.

The transfer function of the table displacement (x_1) to direct disturbance (Fd) and table displacement (x_1) to ground vibration (x_0) can be generated using the following equation

$$\frac{\frac{X_1(s)}{F_d(s)}}{} = \frac{\beta_4 s^4 + \beta_3 s^3 + \beta_2 s^2 + \beta_1 s + \beta_0}{\alpha_7 s^7 + \alpha_6 s^6 + \alpha_5 s^5 + \alpha_4 s^4 + \alpha_3 s^3 + \alpha_2 s^2 + \alpha_1 s + a_0}$$

$$\frac{\frac{X_1(s)}{X_0(s)}}{} = \frac{\gamma_6 s^6 + \gamma_5 s^5 + \gamma_4 s^4 + \gamma_3 s^3 + \gamma_2 s^2 + \gamma_1 s + \gamma_0}{\alpha_7 s^7 + \alpha_6 s^6 + \alpha_5 s^5 + \alpha_4 s^4 + \alpha_3 s^3 + \alpha_2 s^2 + \alpha_1 s + a_0}$$

where

$$\alpha_7 = (m_1 m_2 T + c_1 m_2)$$
$$\alpha_6 = (m_1 m_2 + c_1 k_2 k_{d2} + m_1 T k_2 k_{d2})$$
$$\alpha_5 = (A_0 k_{d1} k_s m_2 + T k_2 k_{p2} m_1 + G_F k_{a1} m_2 + T k_1 m_2 + c_1 k_2 k_{p2} + k_2 k_{d2} m_1 + k_2 k_{d2} m_2 - k_2 k_{p2} m_2 + c_1 m_2)$$
$$\alpha_4 = (A_0 k_{p1} k_s m_2 + G_F k_2 k_{a1} k_{d2} + T k_1 k_2 k_{d2} + T k_2 k_{i2} m_1 + {k_2}^2 {k_{d2}}^2 - {k_2}^2 k_{d2} k_{p2} + c_1 k_2 k_{d2} + c_1 k_2 k_{i2} - k_2 k_{i2} m_2 + k_2 k_{p2} m_1 + k_1 m_2)$$
$$\alpha_3 = ({k_2}^2 k_{d2} k_{p2} + A_0 k_2 k_{d1} k_{p2} k_s + A_0 k_2 k_{d2} k_{p1} k_s + A_0 k_{i1} k_s m_2 + G_F k_2 k_{a1} k_{p2} - {k_2}^2 k_{d2} k_{i2} - {k_2}^2 {k_{p2}}^2 + c_1 k_2 k_{p2} + k_1 k_2 k_{d2} + k_2 k_{i2} m_1)$$
$$\alpha_2 = (A_0 k_2 k_{d1} k_{i2} k_s + A_0 k_2 k_{d2} k_{i1} k_s + A_0 k_2 k_{p1} k_{p2} k_s + G_F k_2 k_{a1} k_{i2} + T k_1 k_2 k_{i2} + {k_2}^2 k_{d2} k_{i2} - 2{k_2}^2 k_{i2} k_{p2} + c_1 k_2 k_{i2} + k_1 k_{p1} k_{p2})$$
$$\alpha_1 = (A_0 k_2 k_{i1} k_{p2} k_s + A_0 k_2 k_{i2} k_{p1} k_s - {k_2}^2 {k_{i2}}^2)$$
$$\alpha_0 = A_0 k_2 k_{i1} k_{i2} k_s$$
$$\beta_5 = T m_2$$
$$\beta_4 = (m_2 + k_2 T k_{d2})$$
$$\beta_3 = (k_2 k_{d2} + k_2 T k_{p2})$$
$$\beta_2 = (k_2 T k_{i2} + k_2 k_{p2})$$
$$\beta_1 = k_2 k_{i2}$$
$$\gamma_6 = T c_1 m_2$$
$$\gamma_5 = (c_1 m_2 + T k_1 m_2 + T c_1 k_2 k_{d2} + A_0 T k_{d1} k_s m_2)$$
$$\gamma_4 = (k_1 m_2 + c_1 k_2 k_{d2} + T k_1 k_2 k_{d2} + T c_1 k_2 k_{p2} + A_0 k_{p1} k_s m_2 + A_0 T k_2 k_{d1} k_{d2} k_s)$$
$$\gamma_3 = (A_0 T k_2 k_{d1} k_{p2} k_s + A_0 T k_2 k_{d2} k_{p1} k_s + A_0 k_{i1} k_s m_2 + T c_1 k_2 k_{i2} + T k_1 k_2 k_{p2} + c_1 k_2 k_{p2} + k_1 k_2 k_{d2})$$
$$\gamma_2 = (A_0 T k_2 k_{d1} k_{i2} k_s + A_0 k_2 k_{d2} k_{i2} k_s + A_0 k_2 k_{p2} k_{p2} k_s + T k_1 k_2 k_{i2} + c_1 k_2 k_{i2} + k_1 k_2 k_{p2})$$
$$\gamma_1 = (A_0 k_2 k_{i1} k_{p2} k_s + A_0 k_2 k_{i2} k_{p1} k_s + k_1 k_2 k_{i2})$$
$$\gamma_0 = A_0 k_2 k_{i1} k_{i2} k_s$$

Equation indicates that an increase in the acceleration feedback gain (k_{a1}) increases the co-efficient of s^6 (α_6), s^5 (α_5) and s^2 (α_2), leading to a significantly greater denominator value compared to the case without acceleration feedback gain. If the denominator increases, the displacement of the table reduces compared to the absence of extra acceleration feedback.

The addition of acceleration feedback effectively increases the table mass. The acceleration feedback coefficient is chosen to ensure the stability of the isolation table. To determine the table's steady-state displacement for direct disturbance, F_d is considered as step function, while the vibration of the base is set to zero (x_0= 0)

$$\frac{X_1(\infty)}{F_d} = \lim_{s \to 0} \frac{\beta_4 s^4 + \beta_3 s^3 + \beta_2 s^2 + \beta_1 s + \beta_0}{\alpha_7 s^7 + \alpha_6 s^6 + \alpha_5 s^5 + \alpha_4 s^4 + \alpha_3 s^3 + \alpha_2 s^2 + \alpha_1 s + a_0}$$

This study uses the pole assignment approach to calculate the controller parameter gains. The designed active vibration isolation system incorporating ADVA with PID control and acceleration feedback results in a seventh-order system. The calculation of acceleration feedback gain for the stated seventh-order system is extremely complex and laborious. Therefore, the isolation table and ADVA are treated as two separate systems, with PID control applied for each of them with additional acceleration feedback for the isolation table.

The isolation table and ADVA are assumed as a one degree of freedom system, where the movement of the table is restricted only in the vertical axis. The fundamental equation of motion for the vibration table can be expressed as follows:

$$m\ddot{x} = F_a + F_d \tag{11}$$

where m represents table mass, x denotes the displacement of the table along the y-axis, F_a, and F_d are the actuating force and direct disturbance on the vibrating table.

The actuating force can be written as

$$F_a = ki_a \quad (12)$$

where k is the actuator force co-efficient and i_a is the actuator current.

Following the Laplace transformation, the dynamics of the isolation table mass can be expressed in the subsequent form

$$X(s) = \left(\frac{k}{ms^2} I(s) + \frac{F_d(s)}{ms^2}\right) \quad (13)$$

where each Laplace transform's variables are represented by identical capital letters.

Controller design

The isolation table's control mechanism employs a PID (proportional, integral, and derivative) controller with acceleration feedback, enabling the control current i(t) can be calculated using the following Laplace-transformed equation:

$$I(s) = -\left(K_{p1} + \frac{K_{i1}}{s} + sK_{d1}\right)\left(X_1(s) - X_0(s)\right) - s^2 K_{a1} X(s) \quad (14)$$

where K_{p1}, K_{i1}, K_{d1} and K_{a1}represent the proportional, integral, derivative, and acceleration feedback gains, respectively

The transfer function that characterises the system's dynamics regarding table displacement due to the on-board disturbances and ground vibrations can be defined by the next two equations

$$\frac{X(s)}{F_d(s)} = \frac{s}{(m + kk_{a1})t_c(s)}$$

$$\frac{X(s)}{X_0(s)} = \frac{kk_{d1}s^2 + kk_{p1}s + kk_{i1}}{(m + kk_{a1})t_c(s)}$$

where t_c(s) is the characteristics equation of the PID-controlled system with acceleration feedback and is expressed as follows:

$$t_c(s) = s^3 + \frac{kk_{d1}}{(m + kk_{a1})}s^2 + \frac{kk_{p1}}{(m + kk_{a1})}s + \frac{kk_{i1}}{(m + kk_{a1})}$$

For the third order system, the characteristic equation can be expressed as follows

$$t_d(s) = (s + \omega_1)(s^2 + 2\zeta_1\omega_2 s + {\omega_2}^2) = s^3 + \lambda_2 s^2 + \lambda_1 s + \lambda_0$$

where $\lambda_2 = 2\zeta_1\omega_2 + \omega_1, \lambda_1 = 2\zeta_1\omega_1\omega_2 + {\omega_2}^2, \lambda_0 = \omega_1{\omega_2}^2$. For simplicity, it is assumed that $\omega_1\omega_2 = \omega_d$.

The dynamics of the second order system are characterised by two variables$\omega_d(2\pi f_d)$ and $\zeta_1 = \zeta_r$which are used to characterize the dynamics of the system. Hence, the controller gains are obtained by means of comparing between the ideal and system characteristics equations.

$$K_{p1} = \frac{\lambda_2(m + kk_{a1})}{k}$$
$$K_{i1} = \frac{\lambda_0(m + kk_{a1})}{k}$$
$$K_{d1} = \frac{\lambda_1(m + kk_{a1})}{k}$$

The transfer function representation for the absorber mass displacement in response to direct disturbance with PID control can be computed using the following equations, derived similar to the isolation table

$$\frac{X(s)}{F_d(s)} = \frac{s}{m\hat{t}_c(s)}$$

where $\hat{t}_c(s)$is the characteristic equation of the absorber dynamic system as expressed by the following equation

$$t_c(s) = s^3 + \frac{kk_{d2}}{m}s^2 + \frac{kk_{p2}}{m}s + \frac{kk_{i2}}{m}$$

where K_{p2}, K_{i2} and $K_{d2}$are the proportional, integral and derivative gain respectively.

The PID controller gains are determined by comparing the characteristic equation with the ideal one, resulting in the following equation.

$$K_{p2} = \frac{\lambda_1 m}{k}, K_{i2} = \frac{\lambda_0 m}{k}, K_{d1} = \frac{\lambda_2 m}{k}$$

Theoretical analysis of controller design suggested that adding acceleration feedback into the controllers significantly enhances the system's virtual mass. This leads to reduced displacement in response to both known and unknown disturbances.

5. Kalman Filter

An accelerometer is typically employed to determine the absolute acceleration of a system. However, industrial servo-type accelerometers likely to be expensive. A more economical solution to this issue is to implement a MEMS accelerometer; yet these devices often generate noisy data in the low-frequency range. The directly measured values of the feedback signal may be complemented by Kalman filter estimations to decrease noise. The Kalman filter functions as a linear quadratic estimating (LQE)

algorithm by evaluating a sequence of data across time while accounting for noise and other defects.

Theory

The state space model of a dynamic system incorporating both process noise and measurement noise can be represented in the following form.

$$\dot{x} = Ax + Bu + Q$$
$$y = Cx + R$$

where x denotes the state variables, A represents the state matrix, B corresponds to the control input, C refers to the measurement matrices, U is the input vector, Q is the process noise vector, and R stands for the measurement noise vector.

The method of estimating the state using the Kalman filter is broken down into two primary steps: forecasting the state and taking corrective action. The output of each stage is sent into the following phase, and this sequence will continue until the final estimate is obtained. The implementation of these processes is accomplished by means of the Kalman filter algorithm, which is divided into two phases: the time update phase and the measurement update category.

Time update

$$x_{k-1} = \psi\hat{x}_{k-1} + Bu$$
$$P_{k-1} = \psi\hat{P}_{k-1}\acute{\psi} + Q$$

Measurement update

$$\hat{x}_k = x_{k-1} + K_k(y_k - Cx_{k-1})$$
$$K_k = (P_{k-1}\acute{C})(CP_{k-1}\acute{C} + R)^{-1}$$
$$\hat{P}_k = (1 - K_kC)\hat{P}_{k-1}$$

The gain of the Kalman Filter denoted by K_k. (x) and $(\hat{x})$ stand for the expected and estimated values of x. For the simulation purposes, the state space model of the developed system can be written as follows.

$$\frac{d}{dt}\begin{bmatrix} x_1 \\ \dot{x}_1 \\ x_2 \\ \dot{x}_2 \\ p \end{bmatrix} = \begin{bmatrix} 0 & 1 & 0 & 0 & 0 \\ -\frac{k_1}{m_1} & -\frac{c_1}{m_1} & 0 & 0 & \frac{A_0}{m_1} \\ 0 & 0 & 0 & 1 & 0 \\ 0 & 0 & 0 & 0 & 0 \\ 0 & 0 & 0 & 0 & -\frac{1}{T} \end{bmatrix}\begin{bmatrix} x_1 \\ \dot{x}_1 \\ x_2 \\ \dot{x}_2 \\ p \end{bmatrix} + \begin{bmatrix} 0 & 0 \\ 0 & -\frac{k_2}{m_2} \\ 0 & 0 \\ 0 & \frac{k_2}{m_2} \\ \frac{k_s}{T} & 0 \end{bmatrix}\begin{bmatrix} i_1 \\ i_2 \end{bmatrix} + \begin{bmatrix} 0 \\ \frac{1}{m_1} \\ 0 \\ 0 \\ 0 \end{bmatrix} f_d$$

6. **Experiment**

Experimental set-up

The developed system's experimental setup is depicted in a photograph in Figure 3. The leaf springs control the translational movement of the table along the vertical axis. In the low-frequency range, an air spring is an actuator; in the high-frequency range, an ADVA acts as a vibration control device. A voice coil motor drives the absorber mass (VCM). The displacement of the absorber mass with respect to the isolation table and the relative movement of the isolation table with respect to the base are measured by eddy-current gap sensors. The control algorithms is implemented using dSpace 1104. Power amplifier is used to power the electromagnet and Voice Coil Motor (VCM). Dynamic signal analyser Hewlett Packard 35670A is used to measure frequency response for both direct and ground vibration. A servo-type accelerometer is used as reference. Ground vibration is generated using piezoelectric actuators which are placed between the base and floor, and the electromagnets under the table cause direct disturbance. Power amplifier is used to power the electromagnet and VCM.

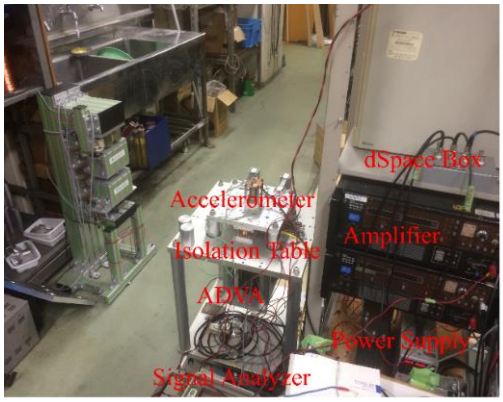

Figure 3. Experimental Set-up

Results and discussion

The dynamic performance characteristics of the developed active vibration isolation system were measured experimentally. To enhance dynamic behaviours such as compliance and transmissibility, additional acceleration feedback was incorporated using PID control. Typically, acceleration is measured using a servo-type accelerometer, which is highly accurate but is expensive. As an alternative, the ADVA used in the developed isolation system can serve both as a vibration control device and as an accelerometer. Additionally, acceleration can be estimated using a Kalman Filter.

To compare acceleration data from the servo-type accelerometer, ADVA-estimated acceleration, and the

Kalman Filter-estimated acceleration, a sinusoidal signal with a frequency of 5 Hz was applied to all the electromagnets beneath the isolation table. The corresponding acceleration data were collected and plotted in Figure 4. The results in Figure 4 indicate that the acceleration estimated from the ADVA control current is much noisier than that from the servo-type accelerometer, and the magnitude of the acceleration differs significantly. To address this, the ADVA acceleration data were calibrated against the servo-type accelerometer data, as shown in Figure 5.

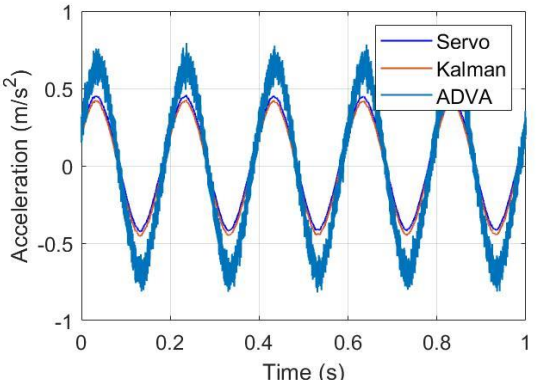

Figure 4. Comparison of the servo, Kalman filter estimated, and ADVA estimated acceleration

To evaluate the impact of Kalman Filter-estimated acceleration feedback on the dynamic characteristics of the isolation table in the frequency domain, several experiments were conducted to measure compliance, which reflects the influence of on-board disturbances on the isolation table's movement. A sweep signal of constant magnitude was applied to the electromagnet beneath the isolation table using a frequency response analyzer, and the displacement of the table was measured using an eddy-current displacement sensor. Simultaneously, the movement of the isolation table and the ADVA mass was controlled using a PID controller. The frequency response was then measured with additional acceleration feedback using both ADVA-estimated acceleration and Kalman Filter-estimated acceleration with PID control. All frequency response results, with and without acceleration feedback, are presented in Figure 6.

The results indicate that acceleration feedback has no effect on very low frequency vibration of the isolation table. However, its effect is significant at the resonance frequency. It is shown that the magnitude of vibration at the resonance peak is -64.65 dB which is reduced to -73.58 dB and further to -80.02 dB due to the ADVA acceleration and Kalman Filter estimated acceleration feedback, respectively. A lower resonance magnitude corresponds to a shorter settling time for the isolation table's vibration. Notably, the reduction in the resonance peak is twice

It is observed that the Kalman Filter-estimated acceleration is less noisy compared to the ADVA-estimated acceleration and does not require for comparison with the servo-type accelerometer data. Therefore, if the state-space model of the developed system is known, Kalman Filter-estimated acceleration can be used as the acceleration feedback signal to improve the dynamic characteristics of the active vibration isolation system.

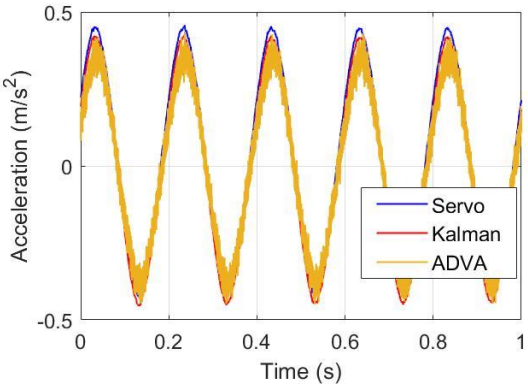

Figure 5. Comparison of the servo, Kalman filter estimated, and calibrated ADVA estimated acceleration

due to the Kalman Filter-estimated acceleration compared to ADVA-estimated acceleration feedback. This implies that the vibration of the isolation table settles in half the time with Kalman Filter feedback compared with the ADVA-estimated feedback.

Likewise, the direct disturbance effect, the transmissibility of ground vibration to the isolation table was measured with additional acceleration feedback. In this case, the ground vibrations were generated by applying voltage to the piezo actuator using a piezo amplifier. The frequency response of the vibration isolation table with additional ADVA-estimated acceleration and Kalman Filter-estimated acceleration feedback, was measured in the same manner as for direct disturbance and summarized in Figure 7. The resonance peak magnitude was reduced from 12 dB to 6 dB due to ADVA-estimated acceleration and further reduced to 3 dB with Kalman filter estimated acceleration. Since the magnitude of ground vibrations is significantly smaller compared to on-board disturbances, the vibration transmitted from the ground to the isolation table is minimal, particularly at higher frequencies, as shown in the high-frequency region of the frequency response. The results in Figure 7 demonstrate that Kalman Filter-estimated acceleration feedback has a greater impact on the vibration isolation characteristics of the table compared to ADVA-estimated acceleration feedback. This superiority is attributed to the Kalman Filter's higher data accuracy and reduced noise.

Due to its low noise and high data accuracy, the Kalman Filter-estimated acceleration feedback enables the developed system to replace servo-type accelerometers. Eliminating the need for servo-type accelerometers significantly reduces the overall cost of the developed active vibration isolation system.

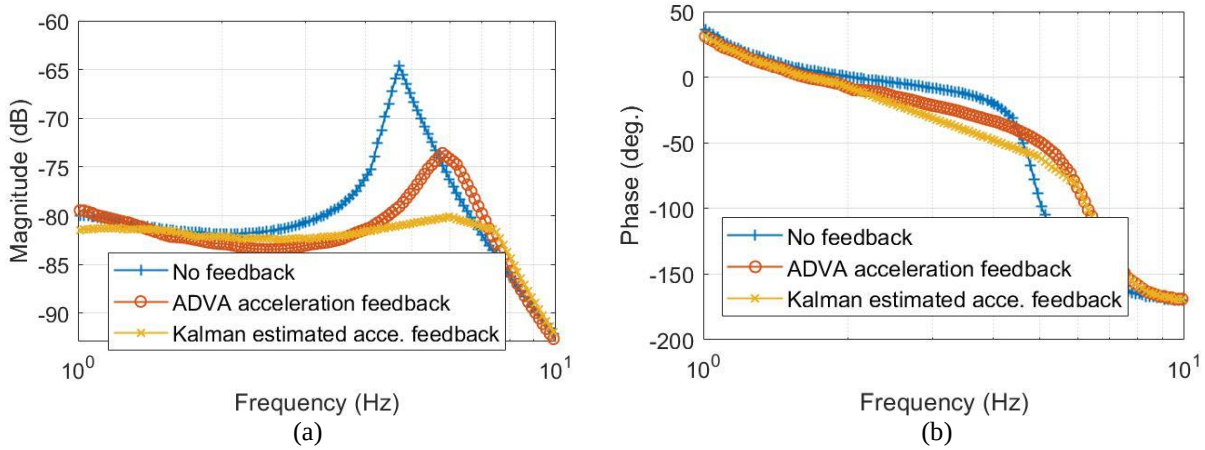

Figure 6. Comparison of compliance of the vibration table with the acceleration feedback (a) mag. (b) phase

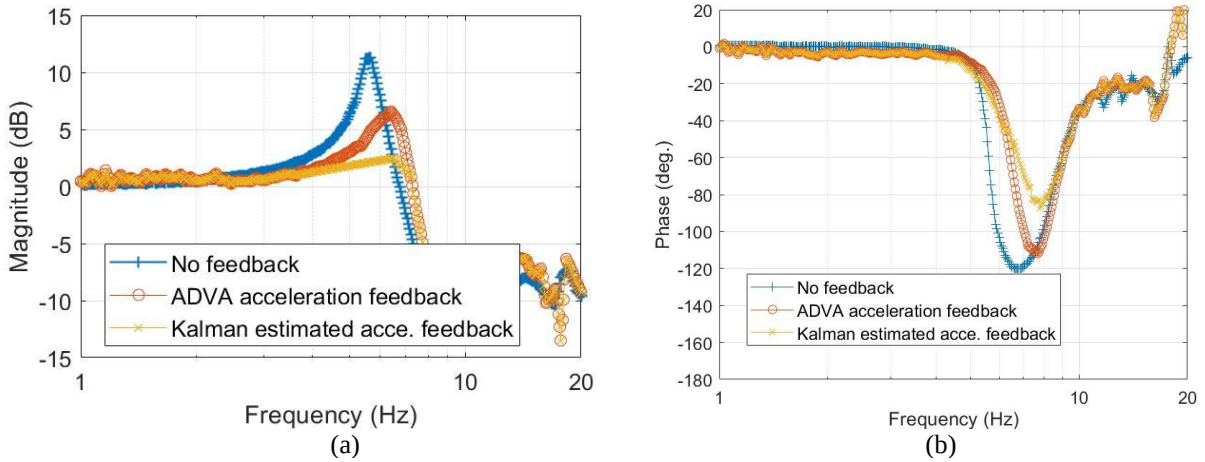

Figure 7. Comparison of transmissibility of the vibration table with the acceleration feedback (a) mag. (b) phase

7. Conclusions

The developed active vibration isolation system utilizes an ADVA that act as accelerometer in low-frequency and controller in high-frequency. By integrating PID control with Kalman Filter-estimated acceleration feedback, the system achieves

- low noise and more accurate acceleration signal as feedback compared to ADVA-acceleration
- a resonance magnitude reduction by factor of two in both compliance and transmissibility characteristics
- eliminates the need for costly servo-type accelerometers, reducing the overall system cost.

References

1. Rivin, E.I., Vibration isolation of precision equipment. Precision engineering, 1995. **17**(1): p. 41-56.
2. Tjepkema, D., J. Van Dijk, and H. Soemers, Sensor fusion for active vibration isolation in precision equipment. Journal of Sound and Vibration, 2012. **331**(4): p. 735-749.
3. Zeng, B., Ultra-Precision Step Stage for Silicon Wafer Scanners.
4. Li, L., et al., Micro-vibration suppression methods and key technologies for high-precision space optical instruments. Acta Astronautica, 2021. **180**: p. 417-428.
5. Qian, Y., et al., Development of active microvibration isolation system for precision space payload. Applied Sciences, 2022. **12**(9): p. 4548.

6. Huang, X. and B. Yang, Towards novel energy shunt inspired vibration suppression techniques: principles, designs and applications. Mechanical Systems and Signal Processing, 2023. **182**: p. 109496.
7. Trumper, D.L. and T. Sato, A vibration isolation platform. Mechatronics, 2002. **12**(2): p. 281-294.
8. Lee, J.H., et al., Control of a hybrid active-passive vibration isolation system. Journal of Mechanical Science and Technology, 2017. **31**: p. 5711-5719.
9. Yoshioka, H., et al., An active microvibration isolation system for hi-tech manufacturing facilities. J. Vib. Acoust., 2001. **123**(2): p. 269-275.
10. Preumont, A. and K. Seto, Active control of structures. 2008: John Wiley & Sons.
11. Qiu, Z.-c., C. Li, and X.-m. Zhang, Experimental study on active vibration control for a kind of two-link flexible manipulator. Mechanical Systems and Signal Processing, 2019. **118**: p. 623-644.
12. Zhang, S., W. He, and D. Huang, Active vibration control for a flexible string system with input backlash. IET Control Theory & Applications, 2016. **10**(7): p. 800-805.
13. Abdeljaber, O., O. Avci, and D.J. Inman, Active vibration control of flexible cantilever plates using piezoelectric materials and artificial neural networks. Journal of sound and Vibration, 2016. **363**: p. 33-53.
14. Liu, C., et al., Recent advances in micro-vibration isolation. Mechanical Systems and Signal Processing, 2015. **56**: p. 55-80.
15. Kerber, F., et al., Control concepts for an active vibration isolation system. Mechanical Systems and Signal Processing, 2007. **21**(8): p. 3042-3059.
16. Müller, T., et al. Modelling and control techniques of an active vibration isolation system. in International Modal Analysis Conference IMAC XXIII. 2005.
17. Liu, C., et al., A review of the inerter and inerter-based vibration isolation: theory, devices, and applications. Journal of the Franklin Institute, 2022. **359**(14): p. 7677-7707.
18. Mizuno, T., et al., Vibration isolation system combining zero-power magnetic suspension with springs. Control Engineering Practice, 2007. **15**(2): p. 187-196.
19. Chen, R., et al., A variable positive-negative stiffness joint with low frequency vibration isolation performance. Measurement, 2021. **185**: p. 110046.
20. Li, H., Y. Li, and J. Li, Negative stiffness devices for vibration isolation applications: a review. Advances in Structural Engineering, 2020. **23**(8): p. 1739-1755.
21. Liu, Y., et al., Dynamic characteristics of quasi-zero stiffness vibration isolation system for coupled dynamic vibration absorber. Archive of Applied Mechanics, 2021. **91**(9): p. 3799-3818.
22. Chang, Y., et al., A quasi-zero-stiffness dynamic vibration absorber. Journal of sound and vibration, 2021. **494**: p. 115859.
23. Yan, B., et al., Active vibration isolation of a system with a distributed parameter isolator using absolute velocity feedback control. Journal of Sound and Vibration, 2010. **329**(10): p. 1601-1614.
24. Watanabe, K., et al. Combination of H/sup/spl infin//and PI control for an electromagnetically levitated vibration isolation system. in Proceedings of 35th IEEE Conference on Decision and Control. 1996. IEEE.
25. Beijen, M., et al., Self-tuning feedforward control for active vibration isolation of precision machines. IFAC Proceedings Volumes, 2014. **47**(3): p. 5611-5616.
26. Daley, S., J. Hätönen, and D. Owens, Active vibration isolation in a "smart spring" mount using a repititive control approach. IFAC Proceedings Volumes, 2005. **38**(1): p. 55-60.
27. Mizuno, T., et al. Realization of acceleration feedback by using an active dynamic vibration absorber as a sensor in a low-frequency region. in 2015 European Control Conference (ECC). 2015. IEEE.
28. Rasid, S.M.R., et al., Design and control of active vibration isolation system with an active dyna 9 vibration absorber operating as accelerometer. Journal of Sound and Vibration, 2019. **438**: p. 175-190.
29. Li, Y., et al., Active vibration and noise control of vibro-acoustic system by using PID controller. Journal of Sound and Vibration, 2015. **348**: p. 57-70.
30. Jin, X., et al., Robust vibration control for active suspension system of in-wheel-motor-driven electric vehicle via μ-synthesis methodology. Journal of Dynamic Systems, Measurement, and Control, 2022. **144**(5): p. 051007.
31. Yan, B., N. Yu, and C. Wu, A state-of-the-art review on low-frequency nonlinear vibration isolation with electromagnetic mechanisms. Applied Mathematics and Mechanics, 2022. **43**(7): p. 1045-1062.
32. Collette, C. and F. Matichard, Sensor fusion methods for high performance active vibration isolation systems. Journal of sound and vibration, 2015. **342**: p. 1-21.
33. Hoque, E. and T. Mizuno, Magnetic levitation technique for active vibration control, in Magnetic Bearings, Theory and Applications. 2010, Citeseer.
34. Jiménez, S., M.O. Cole, and P.S. Keogh, Vibration sensing in smart machine rotors using internal MEMS accelerometers. Journal of Sound and Vibration, 2016. **377**: p. 58-75.
35. Wang, S., et al., A MEMS resonant accelerometer for low-frequency vibration detection. Sensors and Actuators A: Physical, 2018. **283**: p. 151-158.
36. Moschas, F. and S. Stiros, Experimental evaluation of the performance of arrays of MEMS accelerometers. Mechanical Systems and Signal Processing, 2019. **116**: p. 933-942.
37. Yasin, F.M., Measurement of noise characteristics of MEMS accelerometers. 2002, George Washington University.
38. Sasiadek, J.Z., Sensor fusion. Annual Reviews in Control, 2002. **26**(2): p. 203-228.